



29 of population, and 50% of food production of China. Green water from western  
30 provinces is the largest contributor to water resources, while green water from  
31 southwestern and central provinces embodies the highest GDP, population, and food  
32 production. Overall, the embodied socio-economic values of green water flow increase  
33 from source to sink provinces, suggesting that green water from less developed  
34 provinces effectively supports the higher socio-economic status of developed provinces.  
35 The assessment emphasizes the substantial tele-connected socio-economic values of  
36 green water flows and the need to incorporate them toward a more comprehensive and  
37 effective water resources management.

38

## 39 **1 Introduction**

40 Terrestrial moisture recycling is a crucial process of the water cycle, whereby  
41 water evaporates from land into the atmosphere, travels with prevailing winds, and  
42 eventually falls back to the land as precipitation (van der Ent et al., 2010; Keys and  
43 Wang-Erlandsson, 2018; Zemp et al., 2014). Terrestrial evapotranspiration (i.e., green  
44 water) (Falkenmark and Rockström, 2006), which includes evaporation and  
45 transpiration from land and vegetation, contributes to over half of the global  
46 precipitation on land (van der Ent et al., 2010; Theeuwes et al., 2023; Tuinenburg et al.,  
47 2020). Green water flows from upwind source regions to generate precipitation and  
48 supply water resources for the social development of downwind sink regions through  
49 moisture recycling (Schyns et al., 2019; Wang-Erlandsson et al., 2022). Analogous to  
50 the upstream and downstream connection via blue water (referring to surface water and  
51 groundwater flow within a watershed (Gleeson et al., 2020), the upwind source and  
52 downwind sink regions are connected via green water flow within the evaporationshed  
53 (i.e., downwind regions receiving precipitation from a specific location's evaporation)  
54 (Ent and Savenije, 2013). Changes in both blue and green water flow directly impact  
55 water resources availability, thereby influencing regional water security and human  
56 societies (Keys et al., 2019).

57 The blue and green water flows provide a mechanism through which  
58 upstream/upwind changes in ecohydrological and societal processes may affect the  
59 downwind/downstream supply of water resources and, thus, ecological and societal  
60 systems therein. Due to upstream water withdrawal and dams, global total blue water  
61 flow into oceans and internal sinks decreased by 3.5% in 2002 compared to 1961–1990  
62 (Döll et al., 2009). The decline in water availability exacerbated water stress in

63 downstream of transboundary river basins (Munia et al., 2016). Moreover, upstream  
64 vegetation restoration, soil and water conservation practices reduced water yield  
65 downstream, as already happened in the Yellow River (Wang et al., 2017; Zhou et al.,  
66 2015b). Numerous studies have investigated the causal connection of blue water flow  
67 from upstream and downstream regions, yet research into the connection of green water  
68 flow from upwind and downwind regions and their impacts remains inadequate.

69 Unlike blue water flow primarily shaped by terrain with specific routes and  
70 regulated by human activities (e.g., reservoir, transfer), green water flow is transported  
71 by atmospheric air movement in a pervasive manner from evapotranspiration to  
72 precipitation in downwind sink regions (Schyns et al., 2019). This establishes a spatial  
73 linkage between source and sink regions for green water flow through the moisture  
74 recycling process, similar to blue water flow through the surface hydrological process.  
75 Therefore, evapotranspiration changes associated with land cover changes in source  
76 regions are likely to impact not only downstream rivers via blue water flow but also  
77 downwind precipitation via green water flow (Keys et al., 2012), with further  
78 implications on socio-economic development (Wang-Erlandsson et al., 2018). For  
79 example, vegetation greening reduced blue water but increased downwind water  
80 availability globally through green water (Cui et al., 2022). Reduction in green water  
81 in Amazon decreased downwind precipitation in the United States (Lawrence and  
82 Vandecar, 2015), and reduction in green water source regions could decrease potential  
83 crop yields in key global food-producing regions (Bagley et al., 2012).

84 Source regions supply water resources to support sink regions' socio-economic  
85 development through both blue and green water flows. Existing research has  
86 extensively assessed the socio-economic values of blue water, e.g., the population  
87 dependency on runoff (Green et al., 2015; Viviroli et al., 2020), while seldom  
88 considering the tele-connected effects of green water on socio-economy. In fact, green  
89 water is also closely tied to human society because green water traveling from source  
90 regions precipitates, recharges water resources, and ultimately sustains socio-economic  
91 activities, livelihoods, and ecosystems in sink regions (Arag ão, 2012; Keys and Wang-  
92 Erlandsson, 2018; O'Connor et al., 2021). These contributions should be quantified and  
93 recognized as the value of green water to socio-economy, which expands the scope of  
94 water management and water security maintenance (Keys et al., 2017; Rockström et al.,  
95 2023). Emerging moisture tracking technologies offer feasible ways to quantify green  
96 water flow across regions at large scale (Keys et al., 2019; Li et al., 2023; Theeuwens et

97 al., 2023) and pave the way for assessing the socio-economic values of green water.

98 The general spatial and seasonal patterns of moisture flows in China are  
99 determined by regional atmospheric circulation systems, including prevailing westerly  
100 winds (from the west toward the east) in most of China between 30° and 60° (Bridges  
101 et al., 2023), the East Asian monsoon in eastern China, and India monsoon in  
102 southwestern China. In summer, the East Asian and Indian monsoons supply moisture  
103 for precipitation in eastern and southwestern China (Tian and Fan, 2013). In winter, the  
104 East Asian monsoon drives northwesterly moisture transport across much of China and  
105 generates precipitation (Wu and Wang, 2002). Recent studies analyzed the large-spatial  
106 pattern of moisture recycling in China at the grid (Zhang et al., 2023a), river basin  
107 (Wang et al., 2023b), and ecological regions scales (Xie et al., 2024), or for specific  
108 regions (Pranindita et al., 2022; Zhang et al., 2024). However, green water flows from  
109 different regions are interlinked and become sources and sinks of each other. Such green  
110 water transfer at a sub-national scale effectively forms an interconnected green water  
111 flow network. It highlights the mutual dependency of green water and its socio-  
112 economic contributions, especially for large countries like China. Few studies focus on  
113 green water flows at the administrative district scale, which is important for water  
114 management. Furthermore, the substantial regional disparities in socio-economic  
115 development add complexity to understanding the socio-economic contributions of  
116 green water among Chinese provinces. The western provinces with a weak economic  
117 status and sparse populations are abundant in water resources (Ya-Feng et al., 2020). In  
118 contrast, the economically developed and densely populated eastern provinces suffer  
119 from water scarcity (Varis and Vakkilainen, 2001). Therefore, quantifying  
120 interprovincial green water flows and evaluating the embedded socio-economic values  
121 offer new perspectives for optimizing water resource utilization and mitigating the  
122 imbalance in regional socio-economic development.

123 In this study, we used a high-quality moisture trajectory dataset from the UTrack  
124 model to quantify and visualize the interprovincial network of green water flows within  
125 China. Next, we combined socio-economic statistical data to evaluate socio-economic  
126 values embodied in green water flow for economic production, population and food  
127 production. Our study aims to reveal the transboundary green water flows within China  
128 and their tele-connected effects on the socio-economy. This study incorporates green  
129 water flow into water resources, extending water resources management beyond blue  
130 water toward a more complete understanding of the water cycle and its socio-economic

131 implications, which is beneficial to assess and optimize regional water security.

## 132 **2 Data and Methods**

### 133 **2.1 Data**

134 This study used the moisture trajectory dataset generated by the Lagrangian  
135 moisture tracking model “UTrack-atmospheric-moisture” driven by ERA5 reanalysis  
136 data. The model is the state-of-the-art moisture tracking model, producing more  
137 detailed evaporation footprints due to the high spatial resolution and reduced  
138 unnecessary complexity (Tuinenburg and Staal, 2020). The dataset provides monthly  
139 mean moisture flows at the global scale with a spatial resolution of  $0.5^\circ$  for 2008–2017,  
140 expressed as the fractions of evaporation from a source grid allocated to precipitation  
141 at a sink grid (Tuinenburg et al., 2020). It has been widely used in moisture recycling  
142 research with various spatial scales, such as precipitation source of the grid (Staal et al.,  
143 2023; Wei et al., 2024; Zhang et al., 2023a) and basin scale (Wang et al., 2023b), and  
144 moisture transport between nations (Rockström et al., 2023). The moisture trajectory  
145 dataset was used in conjunction with the multi-year monthly mean ET of 2008–2017  
146 from the ERA5 reanalysis dataset to estimate precipitation in a sink grid originating  
147 from a source grid.

148 The socio-economic statistical data in 2008–2017 from the China Statistical  
149 Yearbook were used to estimate the socio-economic values of green water in terms of  
150 water resources volume, gross domestic product (GDP), population, and food  
151 production for 31 provinces in mainland China, without Hong Kong, Macau, and  
152 Taiwan due to the data limitation. GDP was adjusted to price in the year 2020 to  
153 eliminate the effects of inflation.

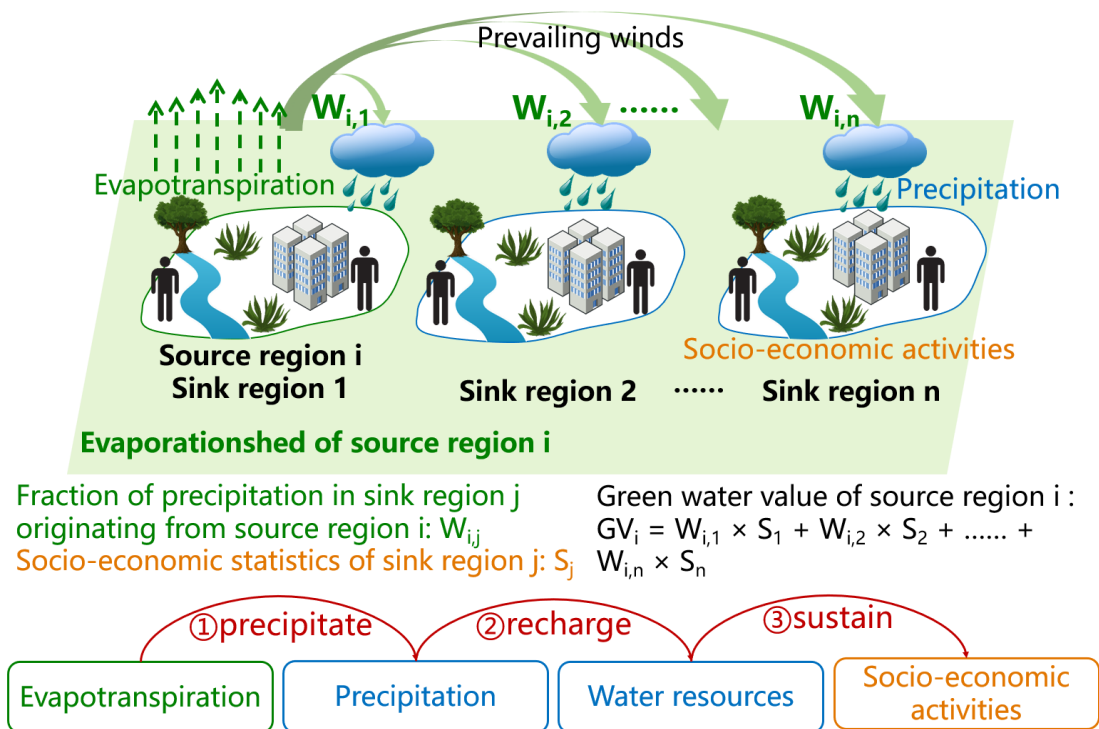
### 154 **2.2 Quantify green water flows in China**

155 We quantified interprovincial moisture flows and their precipitation contribution  
156 following the workflow described in Fig. A1. At each sink grid, the evapotranspiration  
157 (ET) to precipitation (ET-to-P) fractions from the moisture trajectory datasets were  
158 multiplied by ERA5 ET to obtain monthly precipitation contribution by moisture from  
159 its source grids. Repeating the calculation for all grids within a sink province and  
160 summing them up yielded the precipitation in the sink province contributed by each  
161 source grid (Fig. A1 Step 1). Next, we employed zonal statistics to sum up precipitation  
162 in the sink province contributed by grids of each source province, and the precipitation  
163 contribution was converted to relative values, i.e., the fraction of precipitation in sink  
164 province  $j$  originating from green water of a source province  $i$  (denoted as  $W_{ij}$ ) rather

165 than absolute contribution to reduce the uncertainty in the latter (Fig. A1 Step 2). The  
 166 fractions  $W_{ij}$  multiplied by the observed precipitation of the sink province restore the  
 167 absolute precipitation contribution. This practice ensures that provincial precipitation  
 168 is fully decomposed into different sources, reducing the estimation bias of sink  
 169 precipitation due to unclosed water balance by ET and precipitation data (De Petrillo et  
 170 al., 2024). Finally, the interprovincial green water flows in China were derived after  
 171 estimating each province individually.

172 The direction of green water flows can be represented by a vector starting from a  
 173 source to sink province determined by their geometric centers and with its length  
 174 denoting flow magnitude. Since green water flows have multiple destinations, each  
 175 flow points to different sink provinces, and even outside of China. For each source  
 176 province, all of their domestic green water flow vectors can be averaged to a composite  
 177 to represent their net direction and magnitude, which are mainly determined by  
 178 atmospheric wind conditions, source location and green water volume.

179 **2.3 Quantify socio-economic values embodied in green water**



180  
 181 Figure 1. A conceptual diagram depicts the teleconnection of green water flows and their socio-  
 182 economic contributions in a cascade manner. Evapotranspiration (green dotted arrows) from  
 183 source region  $i$  flows downwind with prevailing winds (green thick arrows) and precipitates in  
 184 sink region  $n$ , which recharges water sources and sustains socio-economic activities in sink  
 185 regions.

186 Green water from upwind source provinces flows and precipitates downwind to

187 recharge water resources, and therefore sustains socio-economic activities in sink  
 188 provinces, as depicted in Fig. 1. Consequently, precipitation, water resources, and  
 189 socio-economic factors such as economic activities, human livelihood, and crop  
 190 production in sink provinces rely on green water exported from source provinces.  
 191 Changes in green water may affect water resource volume, and then impact economic  
 192 activities, livelihood, and crop production through water supply. We chose water  
 193 resources volume, economic output (measured by GDP), population, and food  
 194 production as the four socio-economic indicators that are tightly related to water  
 195 resources to evaluate the socio-economic contributions of green water.

196 If we assume all socio-economic activities in sink province  $j$  are sustained by  
 197 precipitation which constitutes water resources and recharges groundwater, socio-  
 198 economic statistics of sink province  $j$  can be partitioned to source provinces by their  
 199 share of precipitation contribution ( $W_{ij}$ ). Therefore, multiplying socio-economic  
 200 statistics in sink province  $j$  ( $S_j$ ) by  $W_{ij}$  yielded the socio-economic value of green water  
 201 from source province  $i$ . The total socio-economic value of green water of source  
 202 province  $i$  ( $GV_i$ ) can be obtained by summing its contributions to all sink provinces (Fig.  
 203 1), as equation (1):

$$204 \quad GV_i = \sum_{j=1}^n (W_{i,j} \times S_j), \quad (1)$$

205 where  $S_j$  is the average socio-economic value of 2008-2017 (i.e., water resources  
 206 volume ( $\text{km}^3$ ), GDP (in unit of CNY, 1 CNY = 0.14 USD), population (persons), and  
 207 food production (ton)) at sink province  $j$ ,  $n$  is the number of sink provinces.

208 Due to the different socio-economic development statuses, the same amount of  
 209 green water may produce different socio-economic values between source and sink  
 210 provinces. This means green water flow also involves changes in embodied socio-  
 211 economic value from source to sink provinces. We used water productivity in the source  
 212 province ( $WP_i$ ) to calculate the socio-economic values of its exported green water in  
 213 the counterfactual scenario when it was all consumed in the source province without  
 214 interprovincial transfer ( $GV'_i$ ) (Eq. 2). The results were compared with the actual green  
 215 water's socio-economic values (Eq. 1) (namely socio-economic values of exported  
 216 green water when it is consumed in sink provinces) as:

$$217 \quad GV'_i = \sum_{j=1}^n (W_{i,j} \times WU_j \times WP_i), \quad (2)$$

218 where  $WU_j$  is water use in sink province  $j$ , and  $WP_i$  is water productivity in source  
 219 province  $i$ . (i.e., economic output, population, and food production per unit water use).

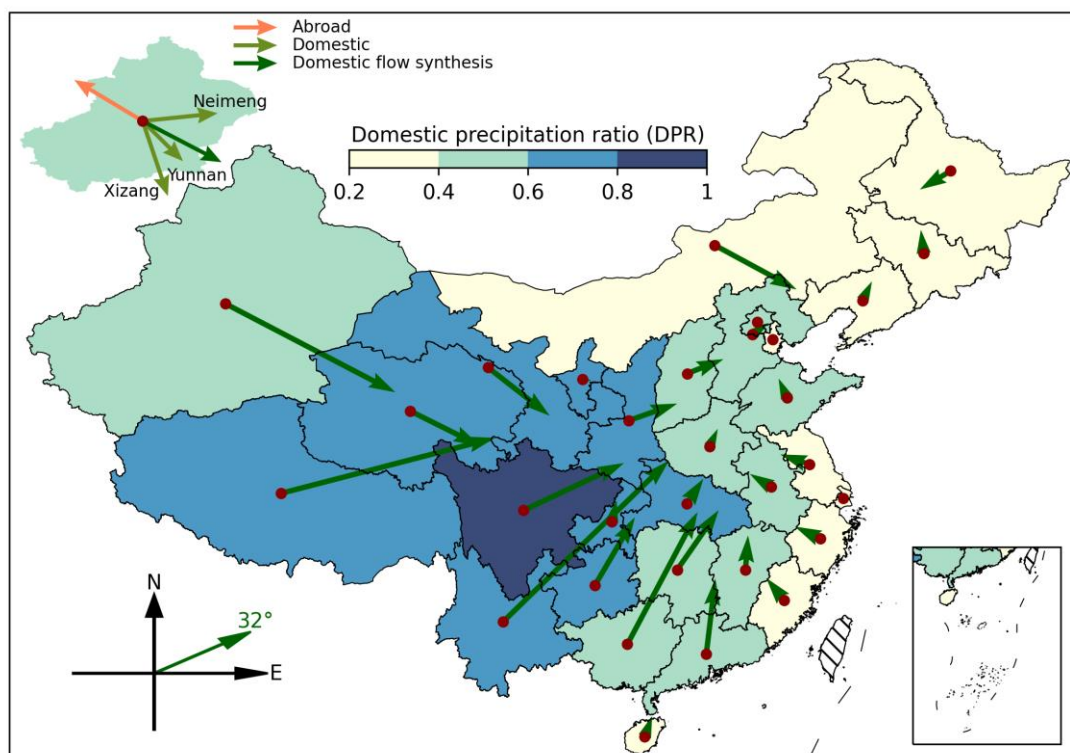
220 The changes in the socio-economic value of green water flow ( $\Delta GV_i$ ) from source





234 different source provinces. Therefore, different provinces in China, acting either as  
 235 sources or sinks, are interconnected through moisture recycling and established an  
 236 interprovincial network (Fig. 2).

237 A large fraction of green water exported from each source province is retained  
 238 locally to generate precipitation (diagonal cells in Fig. 2). The precipitation recycling  
 239 ratio (PRR), the ratio of precipitation generated by local green water to total  
 240 precipitation, reflects how much green water of each source province contributes to its  
 241 own precipitation (Fig. A2c). Xizang has the highest PRR of 0.345, followed by  
 242 Qinghai (0.341) and Sichuan (0.297). Besides local recycling, green water  
 243 predominantly flows and generates more precipitation in neighboring provinces and  
 244 less in distant provinces. For example, green water from Sichuan forms high  
 245 precipitation in neighboring provinces such as Chongqing (138 mm), far surpassing  
 246 other distant sink provinces (< 88 mm).



247  
 248 Figure 3. Direction of green water flows from each source province in China. Green arrows  
 249 indicate the average direction of domestic green water flows, denoted as a vector starting from a  
 250 source (the geometric center in red points) to sink provinces and with its length representing the  
 251 amount of precipitation formed by green water. The face colors on the map represent fractions of  
 252 green water formed precipitation within China of each source province (DPR). The upper left  
 253 corner is a schematic diagram for green water flows from Xinjiang. The lower left corner is the  
 254 composite flow direction of interprovincial green water of all provinces.

255 The direction of interprovincial green water flow can be visualized as a composite

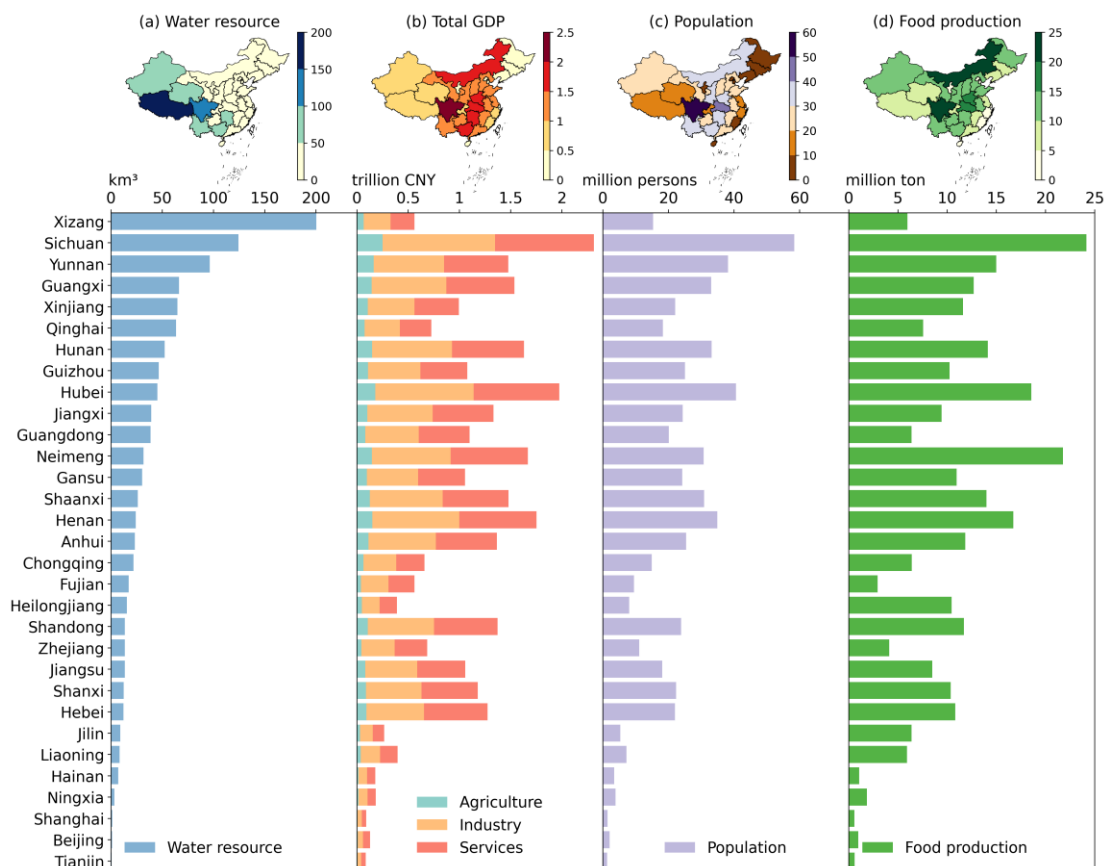
256 direction averaging all domestic green water flows from each source province, which  
257 are mainly determined by atmospheric wind conditions, source location, and green  
258 water volume (Fig. 3). Overall, the average direction of all interprovincial green water  
259 flows is at 32° northeastward (32° north off the east direction), suggesting green water  
260 within China is transported to the north and east directions owing to combined effects  
261 of monsoons and westerly.

262 Green water exported by source provinces contributes to precipitation both within  
263 and outside China. We defined the domestic precipitation ratio (DPR) as the ratio of  
264 green water that formed precipitation in China to each province's total green water  
265 export to represent their relative importance to China's precipitation (Fig. A2a). Green  
266 water from provinces in western and central China mainly flows eastward under the  
267 influence of prevailing westerlies, which extend their evaporationsheds eastward to  
268 cover a large territory of China and generate more precipitation within China (Fig. 3).  
269 For instance, green water from Xizang, the largest exporter in China, produces the  
270 largest domestic precipitation (360 km<sup>3</sup>) (right bar on Fig 2) with a high DPR of 0.74,  
271 contributing to precipitation in other 30 provinces with varying extents (0.2 to 95 mm).  
272 Similarly, the green water from southern provinces is affected by the Indian Ocean  
273 Monsoon (southwest monsoon), which drives green water flowing northeastward. With  
274 a substantial volume of green water, these southern provinces contribute significantly  
275 to domestic precipitation. In contrast, green water from eastern coastal or northwest  
276 border provinces goes to the northwest primarily attributed to the East Asian Monsoon  
277 (southeast monsoon) (Cai et al., 2010). As a result, most evaporationsheds laid outside  
278 China generate less domestic precipitation but more outside the country, resulting in a  
279 lower DPR, such as Fujian (DPR 0.31) and Heilongjiang (DPR 0.23). The northern  
280 provinces are influenced by westerly winds and winter monsoon from Siberia (Sun et  
281 al., 2012), causing predominantly southeastward flow of green water. However,  
282 evaporationsheds of these provinces mainly cover the Pacific Ocean, resulting in a  
283 relatively low DPR despite their substantial volume of exported green water. While  
284 some inland provinces have a high DPR because their evaporationsheds overlap with  
285 mainland China, the low green water volume (Fig. A4) limits their domestic  
286 precipitation contribution (e.g., Gansu and Ningxia with DPR of 0.72 and 0.66,  
287 respectively).

288 Furthermore, precipitation in sink provinces originates from both domestic and  
289 foreign green water sources. Sichuan (337 km<sup>3</sup>), Xizang (298 km<sup>3</sup>), and Qinghai (203

290 km<sup>3</sup>) are the top 3 provinces importing the largest volume of green water from domestic  
 291 sources due to the large ET from themselves and neighboring provinces (top bar of Fig  
 292 2). To quantify the relative importance of domestic sources, we defined the domestic  
 293 source ratio (DSR) in each province as the sum of precipitation contribution from  
 294 domestic sources divided by total precipitation (Fig. A2 (b)). DSR is related to each  
 295 province's precipitationshed (i.e., upwind region contributing evaporation to a specific  
 296 location's precipitation) (Keys et al., 2014) and the included domestic green water  
 297 exporters. The highest DSR found in Qinghai (0.86) and Ningxia (0.82) is because their  
 298 precipitationsheds include large domestic green water exporters like Xinjiang and  
 299 Xizang, which supply considerable green water traveling eastward. Conversely, Hainan  
 300 (0.07) and Guangdong (0.14) in coastal areas have lower DSR because their  
 301 precipitationsheds are primarily located in oceans and other countries due to the  
 302 influence of the summer monsoon (Cai et al., 2010).

### 303 3.2 Socio-economic values embodied in interprovincial green water 304 flows



305  
 306 Figure 4. The embodied socio-economic values of green water flow from source provinces for  
 307 water resources, GDP, population, and food production (average value of 2008-2017) of sink  
 308 provinces in China.

309 Source provinces export green water and create precipitation to sink provinces  
310 through moisture recycling process, recharging water resources and sustaining the  
311 socio-economic development of downwind sink provinces (Fig. 4). The reliance of  
312 socio-economic activities in sink provinces on green water supply from source  
313 provinces implies that the green water and socio-economy are intertwined through the  
314 interprovincial green water flow network, indicating a teleconnection between source  
315 and sink provinces.

316 Our assessment of contribution of green water to water resources indicates that  
317 green water from western provinces recharges the highest volume of water resources.  
318 Xizang (200 km<sup>3</sup>), Sichuan (124 km<sup>3</sup>), and Yunnan (96 km<sup>3</sup>) are the top 3 contributors  
319 of water resources, whose green water export makes up 46%, 51%, and 52% of their  
320 own total water resources, respectively (Table. A1). These regions also correspond to  
321 the top contributors to domestic precipitation, owing to the close linkage between  
322 precipitation and water resources. Although southern and eastern provinces are rich in  
323 water resources due to the wet climate, most of their green water contributes to water  
324 resources outside of China or to the ocean since they are situated downwind of  
325 prevailing westerlies and proximate to the coast (e.g., Guangdong). In total, green water  
326 exported from 31 provinces contributes 43% and 40% of precipitation and water  
327 resources in China (Table. A1).

328 The GDP, population, and food production embodied in green water export from  
329 source provinces are shown in Fig 5b-d, which reflects how much the socio-economy  
330 of downwind sink provinces is supported by green water of source provinces. Overall,  
331 the contribution of green water to selected socio-economic statistics shows similar  
332 rankings because food production and agriculture GDP ( $R = 0.79$ ), population and total  
333 GDP ( $R = 0.85$ ) are spatially correlated (Fig. A6).

334 Sectoral GDP embodied in green water from source provinces is highly related to  
335 the industrial structure in sink provinces. The embodied industry and service sector  
336 GDP values across provinces are relatively comparable, whereas embodied agricultural  
337 GDP values are lower due to the small percentage of agricultural output to total GDP  
338 (Fig. A3).

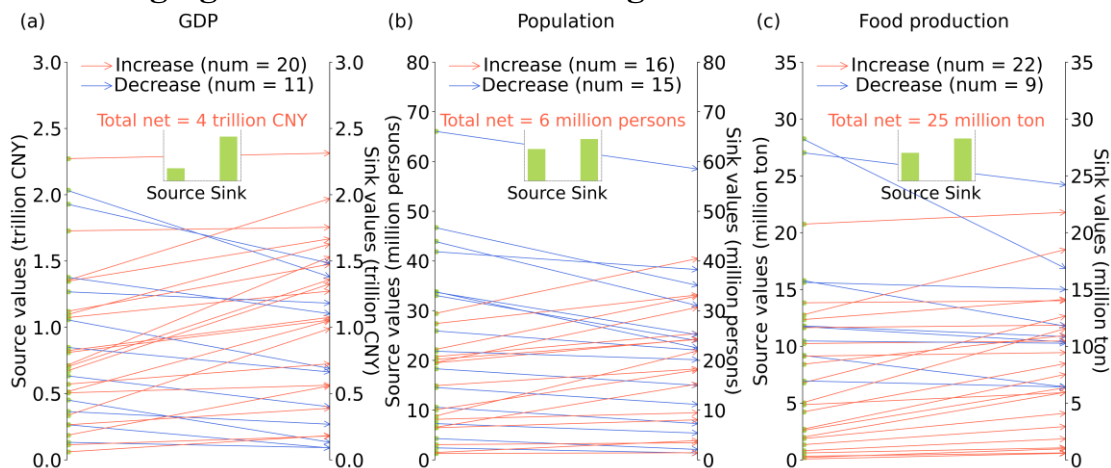
339 Green water from southwest and central provinces (e.g., Sichuan, Hubei, Henan)  
340 embodies the most GDP, population, and food production because of the large  
341 economic volume of these provinces and neighboring regions, as well as the high DPR.  
342 Specifically, green water from Sichuan supports the highest GDP (2.31 trillion CNY),

343 population (58 million persons), and food production (24 million tons) (Table. A2)  
 344 because Sichuan has a high GDP, population, and food production (Fig. A3). Moreover,  
 345 green water from Sichuan contributes significantly to its own precipitation (30%), and  
 346 87% of its green water generates domestic precipitation. These factors together make  
 347 green water in provinces like Sichuan embody the highest socio-economic values.

348 Provinces that export large volumes of green water and have high DPR do not  
 349 necessarily embody more socio-economic values if sink provinces that import their  
 350 green water are less developed. Xizang is the highest green water exporter and the  
 351 largest contributor of water resources (200 km<sup>3</sup>) but ranks low in embodied GDP (0.56  
 352 trillion CNY, 23<sup>rd</sup>), population (15 million, 20<sup>th</sup>), and food production (5.97 million tons,  
 353 23<sup>rd</sup>) because the primary importer of its green water, such as Xizang and Qinghai, have  
 354 low rankings in GDP (31<sup>st</sup>, 30<sup>th</sup>), population (31<sup>st</sup> and 30<sup>th</sup>), and food production (30<sup>th</sup>  
 355 and 29<sup>th</sup>).

356 Green water from highly developed provinces (e.g., southeastern China) may not  
 357 necessarily embody high socio-economic value if they have low DPR. For example,  
 358 Guangdong ranks 1<sup>st</sup> in GDP and population and 17<sup>th</sup> in food production but only has a  
 359 small fraction of green water contributing to domestic precipitation (DPR 0.4). The  
 360 limited domestic precipitation contribution results in low rankings of embodied socio-  
 361 economic values (14<sup>th</sup> for GDP, 17<sup>th</sup> for population, and 21<sup>st</sup> for food production) for  
 362 Guangdong.

### 363 3.3 Changing socio-economic values of green water flows



364  
 365 Figure 5. Changes in socio-economic values embodied in green water flow from source to sink  
 366 provinces for GDP (a), population (b), and food production (c). Thin arrows of different colors  
 367 represent the socio-economic value increase (in red) or decrease (in blue) from source to sink  
 368 provinces. Green bars represent the sum socio-economic value in China's 31 provinces.

369 The substantial socio-economic values embodied in interprovincial green water

370 flows highlight the teleconnection of green water from source provinces and the socio-  
371 economy in sink provinces, including economy, population, and food production. Due  
372 to different socio-economic statuses, the same amount of consumed water resources,  
373 which are recharged by green water, would sustain different socio-economic values  
374 between source and sink provinces. Therefore, the socio-economic values embodied in  
375 green water flow would change when traveling from source to sink provinces. As shown  
376 in Fig. 5, the socio-economic values embodied in green water flow increase from source  
377 to sink provinces by 4 trillion CNY for GDP, 6 million for population, and 25 million  
378 tons for food production, respectively. The increase in the embodied GDP, population,  
379 and food production is observed in 20, 16, and 22 source provinces among a total of 31.  
380 This indicates that green water tends to flow from less to more developed provinces,  
381 sustaining more economic production, population, and food production per unit of  
382 green water. The largest economic output value increases are in Guangxi (+0.83 trillion  
383 CNY, 54%). Xinjiang has the most added value in population (+13 million persons,  
384 59%) and food production (+7 million tons, 60%) because their green water flows to  
385 more developed provinces (Fig. A5). In contrast, decreased socio-economic values of  
386 green water flow are also observed. Shandong, Shaanxi, and Henan have the largest  
387 depreciation in green water values for GDP (-0.66 trillion CNY, 48%), population (-13  
388 million persons, 42%), and food production (-12 million tons, 72%) (Fig. A5) because  
389 their green water flows to provinces with lower socio-economic values.

390 The changing socio-economic values of green water flow reflect the regional  
391 disparity in socio-economic statuses between source and sink provinces. The exported  
392 green water for more than half of the source provinces in China (> 15) has increased  
393 socio-economic values when reaching sink provinces. This shows that green water from  
394 less developed provinces effectively supports the higher socio-economic status of  
395 developed provinces through the interprovincial flow network. Therefore, these  
396 provinces are vitally important green water providers to developed areas. This  
397 teleconnection of green water and socio-economy substantiates that changing land use  
398 in the source provinces that affect evapotranspiration is likely to influence water  
399 resources availability and socio-economic development in the sink provinces (Dias et  
400 al., 2015; Weng et al., 2018). Hence, it is imperative to account for “invisible” green  
401 water flow and its cascade effect in large-scale water resources management.

## 402 **4 Discussion**

403 This study quantified the interprovincial green water flows in China using the

404 moisture recycling framework and a moisture tracking model. The green water flow is  
405 established by transporting evaporated moisture by atmospheric winds from a source  
406 province to precipitate in a sink province. The transferred green water exchanges among  
407 multiple provinces and creates an interprovincial flow network. The location of the  
408 source province and its flow direction largely determine to what extent green water  
409 formed precipitation retains within China. In our estimation, roughly 43% of green  
410 water forms precipitation in China, similar to 44% of PRR identified by Rockström et  
411 al. (2023). The average direction of all interprovincial green water flows in China is  
412 from southwest to northeast, consistent with findings by Xie et al. (2024).

413 Green water flow can fill the gap in land-atmosphere feedback in the traditional  
414 water resources management framework (Keys et al., 2017). Typically, water resources  
415 management only considers blue water changes while neglecting green water flow,  
416 even though the latter may compensate for the former (Hoek van Dijke et al., 2022).  
417 Human activities such as irrigation (Su et al., 2021), afforestation (Li et al., 2018), and  
418 reservoir construction (Biemans et al., 2011; Veldkamp et al., 2017) in upstream regions  
419 may markedly change blue water accessibility in downstream regions. Meanwhile, the  
420 resulting changes of ET in upstream regions (McDermid et al., 2023; Qin, 2021; Shao  
421 et al., 2019) might offset the decline of water resources in downstream by moisture  
422 recycling. Similarly, increased vegetation coverage intercepts more rainfall, reducing  
423 runoff and consequently diminishing water resources availability (Sun et al., 2006;  
424 Zhou et al., 2015a), but the rise of ET may compensate for local and downwind water  
425 availability through increased green water flows (Wang et al., 2023a; Zhang et al.,  
426 2021). Therefore, green water is an essential path of climatic and hydrological  
427 interaction among different regions, providing a new angle for integrated regional  
428 resources management (Keys et al., 2018; te Wierik et al., 2021). A comprehensive  
429 impact assessment of regional water security and optimization would benefit from  
430 combining both blue and green water flows (Schyns et al., 2019) by which  
431 upstream/upwind regions affect regional water resource availability (Creed et al., 2019).

432 With the recognition of the tele-connected effects of green water flows,  
433 maintaining regional water security requires both rational utilization of local water  
434 resources and appropriate land management in the upwind source regions. However,  
435 similar to blue water, water resource management across administrative boundaries has  
436 always been challenging due to conflicting interests among different regions  
437 (Rockström et al., 2023). The diverse strategies developed to enhance regional

438 coordination of blue water management serve as a reference for green water  
439 management, such as the inter-basin water transfer or downstream beneficiaries paying  
440 upstream providers for clean water services (Farley and Costanza, 2010; Pissarra et al.,  
441 2021; Sheng and Webber, 2021). However, unlike blue water resources with well-  
442 established accounting and valuation methods, green water monitoring and valuation  
443 are challenging. Green water from a specific region flows to multiple regions, and the  
444 received green water can subsequently reevaporate and flow to other regions (Zemp et  
445 al., 2014). This interconnected network and cascade complicate the quantification of  
446 how much green water from a source region contributes to human activities in sink  
447 regions. More importantly, it is difficult to measure green water flow through  
448 observations as those measurements made by hydrologic stations for blue water (Hu et  
449 al., 2023; Sheng and Webber, 2021). This study utilized a dataset from a moisture  
450 tracking model to construct an interprovincial green water flow within China, which  
451 offers valuable insights for understanding the quantity of green water flow.

452 Due to the complex dynamics of the green water flow and limitations of the  
453 moisture tracking model, there are still major uncertainties in data and methods of this  
454 study. First, ET and precipitation datasets driving the UTrack model affect the tracked  
455 trajectories and magnitude of moisture flow. The resulting moisture trajectory is  
456 expressed as the ET-to-P fraction, and the exact amount of moisture is restored by the  
457 ET and precipitation datasets chosen by users. Different ET and precipitation datasets  
458 could lead to different precipitation contributions and PRR (Li et al., 2023). We used  
459 the ERA5 dataset to keep consistent with the original UTrack model. It is noted that the  
460 non-closure of the hydrological balance from ERA5 (De Petrillo et al., 2024) and  
461 divergence in moisture tracking models (e.g., simplifications and assumptions) also add  
462 uncertainty and impact the accuracy of the tracked green water flow (Tuinenburg and  
463 Staal, 2020; Zhang et al., 2023b). Moreover, the resulting moisture trajectory data only  
464 represent the climatologically average moisture trajectories and ET (Li et al., 2023),  
465 neglecting the interannual variability in moisture flow trajectory, e.g., those induced by  
466 the influence of extreme weather events or ENSO (Zhao and Zhou, 2021). The  
467 interannual variations in green water flow may affect DPR and DSR in some provinces.  
468 Human adaptation tends to buffer the impacts of interannual variations on the socio-  
469 economy through water resource management such as reservoirs, dams, and other  
470 infrastructure. Accounting for interannual variations in green water flows and their  
471 socio-economic contribution is worth further investigation. Secondly, the socio-



472 economic value assessment of green water in this study only considers green water  
473 flows within China, excluding flows moving abroad and to the ocean that may embody  
474 socio-economic value beyond the territory of mainland China. We mainly attribute  
475 socio-economic values to green water and generated precipitation because precipitation  
476 is the ultimate water source for recharging surface and groundwater of a region. Strictly  
477 speaking, such attribution needs to be more precise because socio-economy also utilizes  
478 streamflow from upstream areas, which deserve separate attention.

479 Moreover, the interactions between blue and green water increase the complexity  
480 to evaluating green water's socio-economic contribution. For example, the blue water  
481 extracted by irrigation increases ET in the source region, providing more moisture for  
482 downwind regions (Yang et al., 2019). Simultaneously, most of the blue water for local  
483 irrigation comes from the green water of upwind regions (McDermid et al., 2023). In  
484 addition, not all water resources replenished by green water-induced precipitation are  
485 accessible for human activities since part of them is used by the natural ecosystem  
486 (Keys et al., 2019). Therefore, it is necessary to distinguish water sources and  
487 consumption to account green water values more accurately. Despite the selected socio-  
488 economic indicators closely linked to water resources, green water flows' socio-  
489 economic contribution can manifest in other aspects such as livestock production and  
490 irrigated agriculture. In future studies, the dynamic linkage between green water, water  
491 resources and economic development can be assessed annually by using a long-term  
492 moisture tracking dataset with a separation of water sources consumed by socio-  
493 economy (surface and groundwater). Nevertheless, our assessment serves as a useful  
494 first step to demonstrate the importance of the tele-connected green water flow in  
495 addition to blue water. Our attempts to quantify the socio-economy embodied in green  
496 water flow fill the gap in green water value assessment and provide a methodological  
497 reference for green water management.

## 498 **5 Conclusion**

499 This study quantified the interprovincial green water flows in China and its tele-  
500 connected effects on the socio-economy. The green water exchanges among different  
501 regions effectively form a complex flow network and embody socio-economic values.  
502 The interprovincial green water in China flows primarily from west to east and to a  
503 lesser extent from south to north, influenced by the co-control of westerlies and  
504 monsoons. Western provinces have significant contributions to precipitation and water  
505 resources in China, while southwestern and central provinces have the most socio-

506 economic values regarding GDP, population, and food production. Green water flowing  
507 from less developed regions supports substantial socio-economic values in more  
508 affluent regions due to disparity in socio-economic development between source and  
509 sink regions. Given the embodied socio-economic benefits of green water, regional  
510 water resources management should consider water flow beyond blue water to integrate  
511 green water for a more comprehensive and effective management of resources and  
512 security. Our study provides a reference for understanding the “invisible” green water  
513 flow and its tele-connected benefits.

#### 514 **Data and code availability**

515 The moisture trajectory dataset is available at  
516 <https://doi.pangaea.de/10.1594/PANGAEA.912710> (Tuinenburg et al., 2020). The  
517 evapotranspiration data from ERA5 reanalysis dataset is available at  
518 [https://cds.climate.copernicus.eu/datasets/reanalysis-era5-single-levels-monthly-](https://cds.climate.copernicus.eu/datasets/reanalysis-era5-single-levels-monthly-means?tab=overview)  
519 [means?tab=overview](https://cds.climate.copernicus.eu/datasets/reanalysis-era5-single-levels-monthly-means?tab=overview) (Hersbach et al., 2023). The socio-economic statistics data is  
520 available from China Statistical Yearbook (<https://data.stats.gov.cn/index.htm>).

521 The Python codes and data used in this study are available at GitHub  
522 (<https://github.com/sangshan-ss/GW-China>).

#### 523 **Author contributions**

524 YL and SS conceived the study and performed data analysis. SS and YL wrote the  
525 manuscript with contributions from CCH, SSZ and HQL.

#### 526 **Competing interests**

527 We declare no conflict of interest of this work.

#### 528 **Financial support**

529 This research was funded by the National Natural Science Foundation of China  
530 (42041007), the Second Tibetan Plateau Scientific Expedition and Research Program  
531 (2019QZKK0405) and the Fundamental Research Funds for the Central Universities.

#### 532 **References**

533 Aragão, L. E. O. C.: The rainforest’s water pump, *Nature*, 489, 217–218,  
534 <https://doi.org/10.1038/nature11485>, 2012.

535 Bagley, J. E., Desai, A. R., Dirmeyer, P. A., and Foley, J. A.: Effects of land cover  
536 change on moisture availability and potential crop yield in the world’s breadbaskets,  
537 *Environ. Res. Lett.*, 7, 014009, <https://doi.org/10.1088/1748-9326/7/1/014009>, 2012.

538 Biemans, H., Haddeland, I., Kabat, P., Ludwig, F., Hutjes, R. W. A., Heinke, J.,  
539 Bloh, W. von, and Gerten, D.: Impact of reservoirs on river discharge and irrigation  
540 water supply during the 20th century, *Water Resources Research*, 47,  
541 <https://doi.org/10.1029/2009WR008929>, 2011.

- 542 Bridges, J. D., Tarduno, J. A., Cottrell, R. D., and Herbert, T. D.: Rapid  
543 strengthening of westerlies accompanied intensification of Northern Hemisphere  
544 glaciation, *Nat Commun*, 14, 3905, <https://doi.org/10.1038/s41467-023-39557-4>, 2023.
- 545 Cai, Y., Tan, L., Cheng, H., An, Z., Edwards, R. L., Kelly, M. J., Kong, X., and  
546 Wang, X.: The variation of summer monsoon precipitation in central China since the  
547 last deglaciation, *Earth and Planetary Science Letters*, 291, 21–31,  
548 <https://doi.org/10.1016/j.epsl.2009.12.039>, 2010.
- 549 Creed, I. F., Jones, J. A., Archer, E., Claassen, M., Ellison, D., McNulty, S. G., van  
550 Noordwijk, M., Vira, B., Wei, X., Bishop, K., Blanco, J. A., Gush, M., Gyawali, D.,  
551 Jobbágy, E., Lara, A., Little, C., Martin-Ortega, J., Mukherji, A., Murdiyarsa, D., Pol,  
552 P. O., Sullivan, C. A., and Xu, J.: Managing Forests for Both Downstream and  
553 Downwind Water, *Front. For. Glob. Change*, 2,  
554 <https://doi.org/10.3389/ffgc.2019.00064>, 2019.
- 555 Cui, J., Lian, X., Huntingford, C., Gimeno, L., Wang, T., Ding, J., He, M., Xu, H.,  
556 Chen, A., Gentine, P., and Piao, S.: Global water availability boosted by vegetation-  
557 driven changes in atmospheric moisture transport, *Nat. Geosci.*, 15, 982–988,  
558 <https://doi.org/10.1038/s41561-022-01061-7>, 2022.
- 559 De Petrillo, E., Fahrländer, S., Tuninetti, M., Andersen, L. S., Monaco, L., Ridolfi,  
560 L., and Laio, F.: Reconciling tracked atmospheric water flows to close the global  
561 freshwater cycle, <https://doi.org/10.21203/rs.3.rs-4177311/v2>, 30 April 2024.
- 562 Dias, L. C. P., Macedo, M. N., Costa, M. H., Coe, M. T., and Neill, C.: Effects of  
563 land cover change on evapotranspiration and streamflow of small catchments in the  
564 Upper Xingu River Basin, Central Brazil, *Journal of Hydrology: Regional Studies*, 4,  
565 108–122, <https://doi.org/10.1016/j.ejrh.2015.05.010>, 2015.
- 566 Döll, P., Fiedler, K., and Zhang, J.: Global-scale analysis of river flow alterations  
567 due to water withdrawals and reservoirs, *Hydrology and Earth System Sciences*, 13,  
568 2413–2432, <https://doi.org/10.5194/hess-13-2413-2009>, 2009.
- 569 Ent, R. J. van der and Savenije, H. H. G.: Oceanic sources of continental  
570 precipitation and the correlation with sea surface temperature, *Water Resources*  
571 *Research*, 49, 3993–4004, <https://doi.org/10.1002/wrcr.20296>, 2013.
- 572 van der Ent, R. J., Savenije, H. H. G., Schaeffli, B., and Steele-Dunne, S. C.: Origin  
573 and fate of atmospheric moisture over continents, *Water Resources Research*, 46,  
574 <https://doi.org/10.1029/2010WR009127>, 2010.
- 575 Falkenmark, M. and Rockström, J.: The New Blue and Green Water Paradigm:  
576 Breaking New Ground for Water Resources Planning and Management, *Journal of*  
577 *Water Resources Planning and Management*, 132, 129–132,  
578 [https://doi.org/10.1061/\(ASCE\)0733-9496\(2006\)132:3\(129\)](https://doi.org/10.1061/(ASCE)0733-9496(2006)132:3(129)), 2006.
- 579 Farley, J. and Costanza, R.: Payments for ecosystem services: From local to global,  
580 *Ecological Economics*, 69, 2060–2068, <https://doi.org/10.1016/j.ecolecon.2010.06.010>,  
581 2010.
- 582 Gleeson, T., Wang-Erlandsson, L., Zipper, S. C., Porkka, M., Jaramillo, F., Gerten,  
583 D., Fetzer, I., Cornell, S. E., Piemontese, L., Gordon, L. J., Rockström, J., Oki, T.,  
584 Sivapalan, M., Wada, Y., Brauman, K. A., Flörke, M., Bierkens, M. F. P., Lehner, B.,  
585 Keys, P., Kummu, M., Wagener, T., Dadson, S., Troy, T. J., Steffen, W., Falkenmark,  
586 M., and Famiglietti, J. S.: The Water Planetary Boundary: Interrogation and Revision,  
587 *One Earth*, 2, 223–234, <https://doi.org/10.1016/j.oneear.2020.02.009>, 2020.

588 Green, P. A., Vörösmarty, C. J., Harrison, I., Farrell, T., Sáenz, L., and Fekete, B.  
589 M.: Freshwater ecosystem services supporting humans: Pivoting from water crisis to  
590 water solutions, *Global Environmental Change*, 34, 108–118,  
591 <https://doi.org/10.1016/j.gloenvcha.2015.06.007>, 2015.

592 Hersbach, H., Bell, B., Berrisford, P., Biavati, G., Horányi, A., Muñoz Sabater, J.,  
593 Nicolas, J., Peubey, C., Radu, R., Rozum, I., Schepers, D., Simmons, A., Soci, C., Dee,  
594 D., and Thépaut, J.-N.: ERA5 monthly averaged data on single levels from 1940 to  
595 present, Copernicus Climate Change Service (C3S) Climate Data Store (CDS),  
596 <https://doi.org/10.24381/CDS.F17050D7>, 2023. (Accessed on 28-10-2024)

597 Hoek van Dijke, A. J., Herold, M., Mallick, K., Benedict, I., Machwitz, M., Schlerf,  
598 M., Pranindita, A., Theeuwes, J. J. E., Bastin, J.-F., and Teuling, A. J.: Shifts in regional  
599 water availability due to global tree restoration, *Nat. Geosci.*, 15, 363–368,  
600 <https://doi.org/10.1038/s41561-022-00935-0>, 2022.

601 Hu, H., Tian, G., Wu, Z., and Xia, Q.: Cross-regional ecological compensation  
602 under the composite index of water quality and quantity: A case study of the Yellow  
603 River Basin, *Environmental Research*, 238, 117152,  
604 <https://doi.org/10.1016/j.envres.2023.117152>, 2023.

605 Keys, P. W. and Wang-Erlandsson, L.: On the social dynamics of moisture  
606 recycling, *Earth System Dynamics*, 9, 829–847, [https://doi.org/10.5194/esd-9-829-](https://doi.org/10.5194/esd-9-829-2018)  
607 2018, 2018.

608 Keys, P. W., van der Ent, R. J., Gordon, L. J., Hoff, H., Nikoli, R., and Savenije,  
609 H. H. G.: Analyzing precipitationsheds to understand the vulnerability of rainfall  
610 dependent regions, *Biogeosciences*, 9, 733–746, [https://doi.org/10.5194/bg-9-733-](https://doi.org/10.5194/bg-9-733-2012)  
611 2012, 2012.

612 Keys, P. W., Barnes, E. A., van der Ent, R. J., and Gordon, L. J.: Variability of  
613 moisture recycling using a precipitationshed framework, *Hydrology and Earth System  
614 Sciences*, 18, 3937–3950, <https://doi.org/10.5194/hess-18-3937-2014>, 2014.

615 Keys, P. W., Wang-Erlandsson, L., Gordon, L. J., Galaz, V., and Ebbesson, J.:  
616 Approaching moisture recycling governance, *Global Environmental Change*, 45, 15–  
617 23, <https://doi.org/10.1016/j.gloenvcha.2017.04.007>, 2017.

618 Keys, P. W., Wang-Erlandsson, L., and Gordon, L. J.: Megacity precipitationsheds  
619 reveal tele-connected water security challenges, *PLOS ONE*, 13, e0194311,  
620 <https://doi.org/10.1371/journal.pone.0194311>, 2018.

621 Keys, P. W., Porkka, M., Wang-Erlandsson, L., Fetzer, I., Gleeson, T., and Gordon,  
622 L. J.: Invisible water security: Moisture recycling and water resilience, *Water Security*,  
623 8, 100046, <https://doi.org/10.1016/j.wasec.2019.100046>, 2019.

624 Lawrence, D. and Vandecar, K.: Effects of tropical deforestation on climate and  
625 agriculture, *Nature Clim Change*, 5, 27–36, <https://doi.org/10.1038/nclimate2430>, 2015.

626 Li, Y., Piao, S., Li, L. Z. X., Chen, A., Wang, X., Ciais, P., Huang, L., Lian, X.,  
627 Peng, S., Zeng, Z., Wang, K., and Zhou, L.: Divergent hydrological response to large-  
628 scale afforestation and vegetation greening in China, *Science Advances*, 4, eaar4182,  
629 <https://doi.org/10.1126/sciadv.aar4182>, 2018.

630 Li, Y., Xu, R., Yang, K., Liu, Y., Wang, S., Zhou, S., Yang, Z., Feng, X., He, C.,  
631 Xu, Z., and Zhao, W.: Contribution of Tibetan Plateau ecosystems to local and remote  
632 precipitation through moisture recycling, *Global Change Biology*, 29, 702–718,  
633 <https://doi.org/10.1111/gcb.16495>, 2023.

- 634 McDermid, S., Nocco, M., Lawston-Parker, P., Keune, J., Pokhrel, Y., Jain, M.,  
635 Jägermeyr, J., Brocca, L., Massari, C., Jones, A. D., Vahmani, P., Thiery, W., Yao, Y.,  
636 Bell, A., Chen, L., Dorigo, W., Hanasaki, N., Jasechko, S., Lo, M.-H., Mahmood, R.,  
637 Mishra, V., Mueller, N. D., Niyogi, D., Rabin, S. S., Sloat, L., Wada, Y., Zappa, L., Chen,  
638 F., Cook, B. I., Kim, H., Lombardozzi, D., Polcher, J., Ryu, D., Santanello, J., Satoh,  
639 Y., Seneviratne, S., Singh, D., and Yokohata, T.: Irrigation in the Earth system, *Nat Rev*  
640 *Earth Environ*, <https://doi.org/10.1038/s43017-023-00438-5>, 2023.
- 641 Munia, H., Guillaume, J. H. A., Mirumachi, N., Porkka, M., Wada, Y., and Kummu,  
642 M.: Water stress in global transboundary river basins: significance of upstream water  
643 use on downstream stress, *Environ. Res. Lett.*, 11, 014002,  
644 <https://doi.org/10.1088/1748-9326/11/1/014002>, 2016.
- 645 O'Connor, J. C., Dekker, S. C., Staal, A., Tuinenburg, O. A., Rebel, K. T., and  
646 Santos, M. J.: Forests buffer against variations in precipitation, *Global Change Biology*,  
647 27, 4686–4696, <https://doi.org/10.1111/gcb.15763>, 2021.
- 648 Pissarra, T. C. T., Sanches Fernandes, L. F., and Pacheco, F. A. L.: Production of  
649 clean water in agriculture headwater catchments: A model based on the payment for  
650 environmental services, *Science of The Total Environment*, 785, 147331,  
651 <https://doi.org/10.1016/j.scitotenv.2021.147331>, 2021.
- 652 Pranindita, A., Wang-Erlandsson, L., Fetzer, I., and Teuling, A. J.: Moisture  
653 recycling and the potential role of forests as moisture source during European  
654 heatwaves, *Clim Dyn*, 58, 609–624, <https://doi.org/10.1007/s00382-021-05921-7>, 2022.
- 655 Qin, Y.: Global competing water uses for food and energy, *Environ. Res. Lett.*, 16,  
656 064091, <https://doi.org/10.1088/1748-9326/ac06fa>, 2021.
- 657 Rockström, J., Mazzucato, M., Andersen, L. S., Fahrländer, S. F., and Gerten, D.:  
658 Why we need a new economics of water as a common good, *Nature*, 615, 794–797,  
659 <https://doi.org/10.1038/d41586-023-00800-z>, 2023.
- 660 Schyns, J. F., Hoekstra, A. Y., Booij, M. J., Hogeboom, R. J., and Mekonnen, M.  
661 M.: Limits to the world's green water resources for food, feed, fiber, timber, and  
662 bioenergy, *Proceedings of the National Academy of Sciences*, 116, 4893–4898,  
663 <https://doi.org/10.1073/pnas.1817380116>, 2019.
- 664 Shao, R., Zhang, B., Su, T., Long, B., Cheng, L., Xue, Y., and Yang, W.: Estimating  
665 the Increase in Regional Evaporative Water Consumption as a Result of Vegetation  
666 Restoration Over the Loess Plateau, China, *Journal of Geophysical Research:*  
667 *Atmospheres*, 124, 11783–11802, <https://doi.org/10.1029/2019JD031295>, 2019.
- 668 Sheng, J. and Webber, M.: Incentive coordination for transboundary water  
669 pollution control: The case of the middle route of China's South-North water Transfer  
670 Project, *Journal of Hydrology*, 598, 125705,  
671 <https://doi.org/10.1016/j.jhydrol.2020.125705>, 2021.
- 672 Staal, A., Koren, G., Tejada, G., and Gatti, L. V.: Moisture origins of the Amazon  
673 carbon source region, *Environ. Res. Lett.*, 18, 044027, <https://doi.org/10.1088/1748-9326/acc676>, 2023.
- 675 Su, Y., Li, X., Feng, M., Nian, Y., Huang, L., Xie, T., Zhang, K., Chen, F., Huang,  
676 W., Chen, J., and Chen, F.: High agricultural water consumption led to the continued  
677 shrinkage of the Aral Sea during 1992–2015, *Science of The Total Environment*, 777,  
678 145993, <https://doi.org/10.1016/j.scitotenv.2021.145993>, 2021.
- 679 Sun, G., Zhou, G., Zhang, Z., Wei, X., McNulty, S. G., and Vose, J. M.: Potential

- 680 water yield reduction due to forestation across China, *Journal of Hydrology*, 328, 548–  
681 558, <https://doi.org/10.1016/j.jhydrol.2005.12.013>, 2006.
- 682 Sun, Y., Clemens, S. C., Morrill, C., Lin, X., Wang, X., and An, Z.: Influence of  
683 Atlantic meridional overturning circulation on the East Asian winter monsoon, *Nature*  
684 *Geosci*, 5, 46–49, <https://doi.org/10.1038/ngeo1326>, 2012.
- 685 Theeuwens, J. J. E., Staal, A., Tuinenburg, O. A., Hamelers, B. V. M., and Dekker,  
686 S. C.: Local moisture recycling across the globe, *Hydrology and Earth System Sciences*,  
687 27, 1457–1476, <https://doi.org/10.5194/hess-27-1457-2023>, 2023.
- 688 Tian, B. and Fan, K.: Factors favorable to frequent extreme precipitation in the  
689 upper Yangtze River Valley, *Meteorol Atmos Phys*, 121, 189–197,  
690 <https://doi.org/10.1007/s00703-013-0261-9>, 2013.
- 691 Tuinenburg, O. A. and Staal, A.: Tracking the global flows of atmospheric  
692 moisture and associated uncertainties, *Hydrology and Earth System Sciences*, 24,  
693 2419–2435, <https://doi.org/10.5194/hess-24-2419-2020>, 2020.
- 694 Tuinenburg, O. A., Theeuwens, J. J. E., and Staal, A.: High-resolution global  
695 atmospheric moisture connections from evaporation to precipitation, *Earth System*  
696 *Science Data*, 12, 3177–3188, <https://doi.org/10.5194/essd-12-3177-2020>, 2020.
- 697 Varis, O. and Vakkilainen, P.: China’s 8 challenges to water resources management  
698 in the first quarter of the 21st Century, *Geomorphology*, 41, 93–104,  
699 [https://doi.org/10.1016/S0169-555X\(01\)00107-6](https://doi.org/10.1016/S0169-555X(01)00107-6), 2001.
- 700 Veldkamp, T. I. E., Wada, Y., Aerts, J. C. J. H., Döll, P., Gosling, S. N., Liu, J.,  
701 Masaki, Y., Oki, T., Ostberg, S., Pokhrel, Y., Satoh, Y., Kim, H., and Ward, P. J.: Water  
702 scarcity hotspots travel downstream due to human interventions in the 20th and 21st  
703 century, *Nat Commun*, 8, 15697, <https://doi.org/10.1038/ncomms15697>, 2017.
- 704 Viviroli, D., Kumm, M., Meybeck, M., Kallio, M., and Wada, Y.: Increasing  
705 dependence of lowland populations on mountain water resources, *Nat Sustain*, 3, 917–  
706 928, <https://doi.org/10.1038/s41893-020-0559-9>, 2020.
- 707 Wang, S., Fu, B., Liang, W., Liu, Y., and Wang, Y.: Driving forces of changes in  
708 the water and sediment relationship in the Yellow River, *Science of The Total*  
709 *Environment*, 576, 453–461, <https://doi.org/10.1016/j.scitotenv.2016.10.124>, 2017.
- 710 Wang, X., Zhang, Z., Zhang, B., Tian, L., Tian, J., Arnault, J., Kunstmann, H., and  
711 He, C.: Quantifying the Impact of Land Use and Land Cover Change on Moisture  
712 Recycling With Convection-Permitting WRF-Tagging Modeling in the Agro-Pastoral  
713 Ecotone of Northern China, *Journal of Geophysical Research: Atmospheres*, 128,  
714 e2022JD038421, <https://doi.org/10.1029/2022JD038421>, 2023a.
- 715 Wang, Y., Liu, X., Zhang, D., and Bai, P.: Tracking Moisture Sources of  
716 Precipitation Over China, *Journal of Geophysical Research: Atmospheres*, 128,  
717 e2023JD039106, <https://doi.org/10.1029/2023JD039106>, 2023b.
- 718 Wang-Erlandsson, L., Fetzer, I., Keys, P. W., van der Ent, R. J., Savenije, H. H. G.,  
719 and Gordon, L. J.: Remote land use impacts on river flows through atmospheric  
720 teleconnections, *Hydrology and Earth System Sciences*, 22, 4311–4328,  
721 <https://doi.org/10.5194/hess-22-4311-2018>, 2018.
- 722 Wang-Erlandsson, L., Tobian, A., van der Ent, R. J., Fetzer, I., te Wierik, S., Porkka,  
723 M., Staal, A., Jaramillo, F., Dahlmann, H., Singh, C., Greve, P., Gerten, D., Keys, P. W.,  
724 Gleeson, T., Cornell, S. E., Steffen, W., Bai, X., and Rockström, J.: A planetary

- 725 boundary for green water, *Nat Rev Earth Environ*, 3, 380–392,  
726 <https://doi.org/10.1038/s43017-022-00287-8>, 2022.
- 727 Wei, F., Wang, S., Fu, B., Li, Y., Huang, Y., Zhang, W., and Fensholt, R.:  
728 Quantifying the precipitation supply of China's drylands through moisture recycling,  
729 *Agricultural and Forest Meteorology*, 352, 110034,  
730 <https://doi.org/10.1016/j.agrformet.2024.110034>, 2024.
- 731 Weng, W., Luedeke, M. K. B., Zemp, D. C., Lakes, T., and Kropp, J. P.: Aerial and  
732 surface rivers: downwind impacts on water availability from land use changes in  
733 Amazonia, *Hydrology and Earth System Sciences*, 22, 911–927,  
734 <https://doi.org/10.5194/hess-22-911-2018>, 2018.
- 735 te Wierik, S. A., Cammeraat, E. L. H., Gupta, J., and Artzy-Randrup, Y. A.:  
736 Reviewing the Impact of Land Use and Land-Use Change on Moisture Recycling and  
737 Precipitation Patterns, *Water Resources Research*, 57, e2020WR029234,  
738 <https://doi.org/10.1029/2020WR029234>, 2021.
- 739 Wu, B. and Wang, J.: Winter Arctic Oscillation, Siberian High and East Asian  
740 Winter Monsoon, *Geophysical Research Letters*, 29, 3-1-3-4,  
741 <https://doi.org/10.1029/2002GL015373>, 2002.
- 742 Xie, D., Zhang, Y., Zhang, M., Tian, Y., Cao, Y., Mei, Y., Liu, S., and Zhong, D.:  
743 Hydrological impacts of vegetation cover change in China through terrestrial moisture  
744 recycling, *Science of The Total Environment*, 915, 170015,  
745 <https://doi.org/10.1016/j.scitotenv.2024.170015>, 2024.
- 746 Ya-Feng, Z., Min, D., Ya-Jing, L., and Yao, R.: Evolution characteristics and policy  
747 implications of new urbanization in provincial capital cities in Western China, *PLoS*  
748 *ONE*, 15, e0233555, <https://doi.org/10.1371/journal.pone.0233555>, 2020.
- 749 Yang, Z., Qian, Y., Liu, Y., Berg, L. K., Hu, H., Dominguez, F., Yang, B., Feng, Z.,  
750 Gustafson Jr, W. I., Huang, M., and Tang, Q.: Irrigation Impact on Water and Energy  
751 Cycle During Dry Years Over the United States Using Convection-Permitting WRF and  
752 a Dynamical Recycling Model, *Journal of Geophysical Research: Atmospheres*, 124,  
753 11220–11241, <https://doi.org/10.1029/2019JD030524>, 2019.
- 754 Zemp, D. C., Schleussner, C.-F., Barbosa, H. M. J., van der Ent, R. J., Donges, J.  
755 F., Heinke, J., Sampaio, G., and Rammig, A.: On the importance of cascading moisture  
756 recycling in South America, *Atmospheric Chemistry and Physics*, 14, 13337–13359,  
757 <https://doi.org/10.5194/acp-14-13337-2014>, 2014.
- 758 Zhang, B., Tian, L., Zhao, X., and Wu, P.: Feedbacks between vegetation  
759 restoration and local precipitation over the Loess Plateau in China, *Sci. China Earth*  
760 *Sci.*, 64, 920–931, <https://doi.org/10.1007/s11430-020-9751-8>, 2021.
- 761 Zhang, B., Gao, H., and Wei, J.: Identifying potential hotspots for atmospheric  
762 water resource management and source-sink analysis, *CSB*, 68, 2678–2689,  
763 <https://doi.org/10.1360/TB-2022-1275>, 2023a.
- 764 Zhang, C., Chen, D., Tang, Q., and Huang, J.: Fate and Changes in Moisture  
765 Evaporated From the Tibetan Plateau (2000–2020), *Water Resources Research*, 59,  
766 e2022WR034165, <https://doi.org/10.1029/2022WR034165>, 2023b.
- 767 Zhang, C., Zhang, X., Tang, Q., Chen, D., Huang, J., Wu, S., and Liu, Y.:  
768 Quantifying precipitation moisture contributed by different atmospheric circulations  
769 across the Tibetan Plateau, *Journal of Hydrology*, 628, 130517,  
770 <https://doi.org/10.1016/j.jhydrol.2023.130517>, 2024.

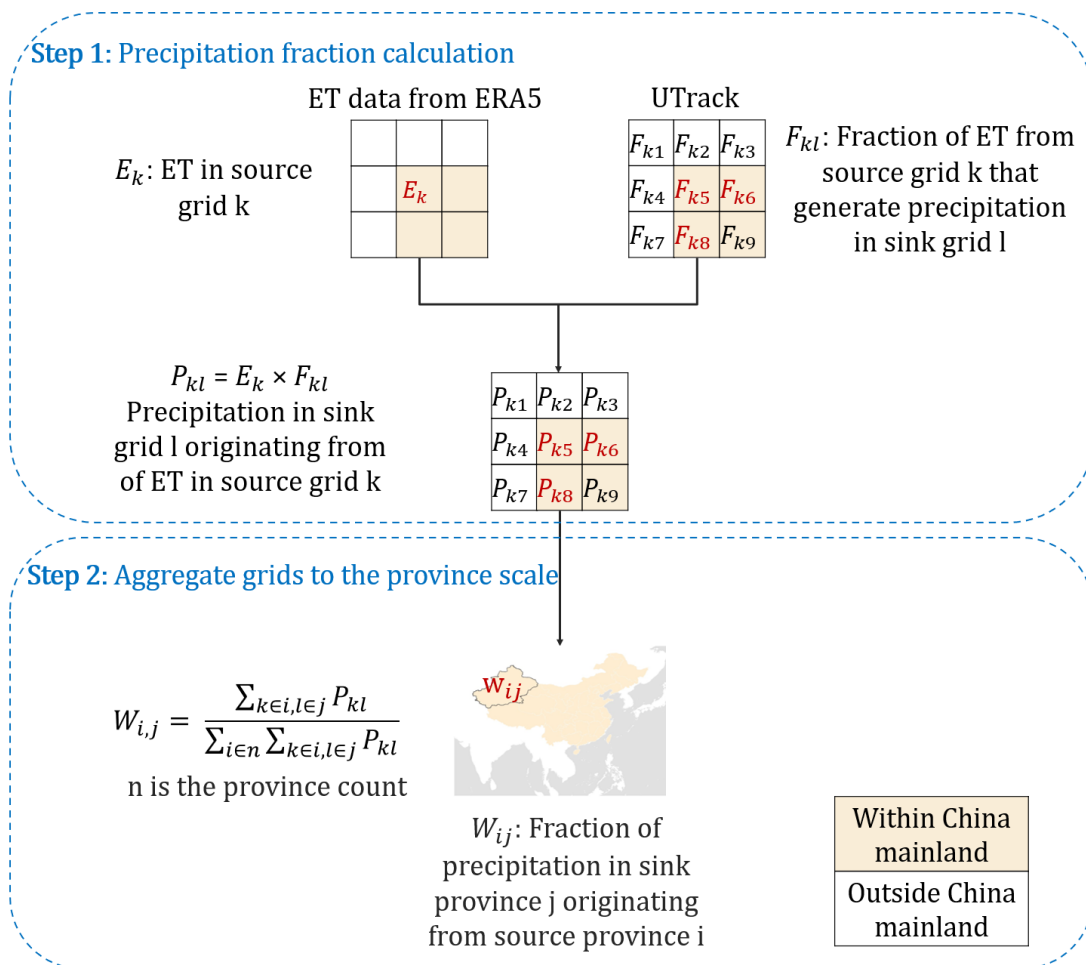
771 Zhao, Y. and Zhou, T.: Interannual Variability of Precipitation Recycle Ratio Over  
 772 the Tibetan Plateau, *Journal of Geophysical Research: Atmospheres*, 126,  
 773 e2020JD033733, <https://doi.org/10.1029/2020JD033733>, 2021.

774 Zhou, G., Wei, X., Chen, X., Zhou, P., Liu, X., Xiao, Y., Sun, G., Scott, D. F., Zhou,  
 775 S., Han, L., and Su, Y.: Global pattern for the effect of climate and land cover on water  
 776 yield, *Nat Commun*, 6, 5918, <https://doi.org/10.1038/ncomms6918>, 2015a.

777 Zhou, Y., Huang, H. Q., Nanson, G. C., Huang, C., and Liu, G.: Progradation of  
 778 the Yellow (Huanghe) River delta in response to the implementation of a basin-scale  
 779 water regulation program, *Geomorphology*, 243, 65–74,  
 780 <https://doi.org/10.1016/j.geomorph.2015.04.023>, 2015b.

781

782 **Appendix A**



783

784 **Figure A1.** Workflow of estimating green water flow. Step 1: calculate precipitation in sink grids

785 originating from ET in source grids. Step 2: calculate the fraction of precipitation in sink

786 provinces originating from source provinces.

787



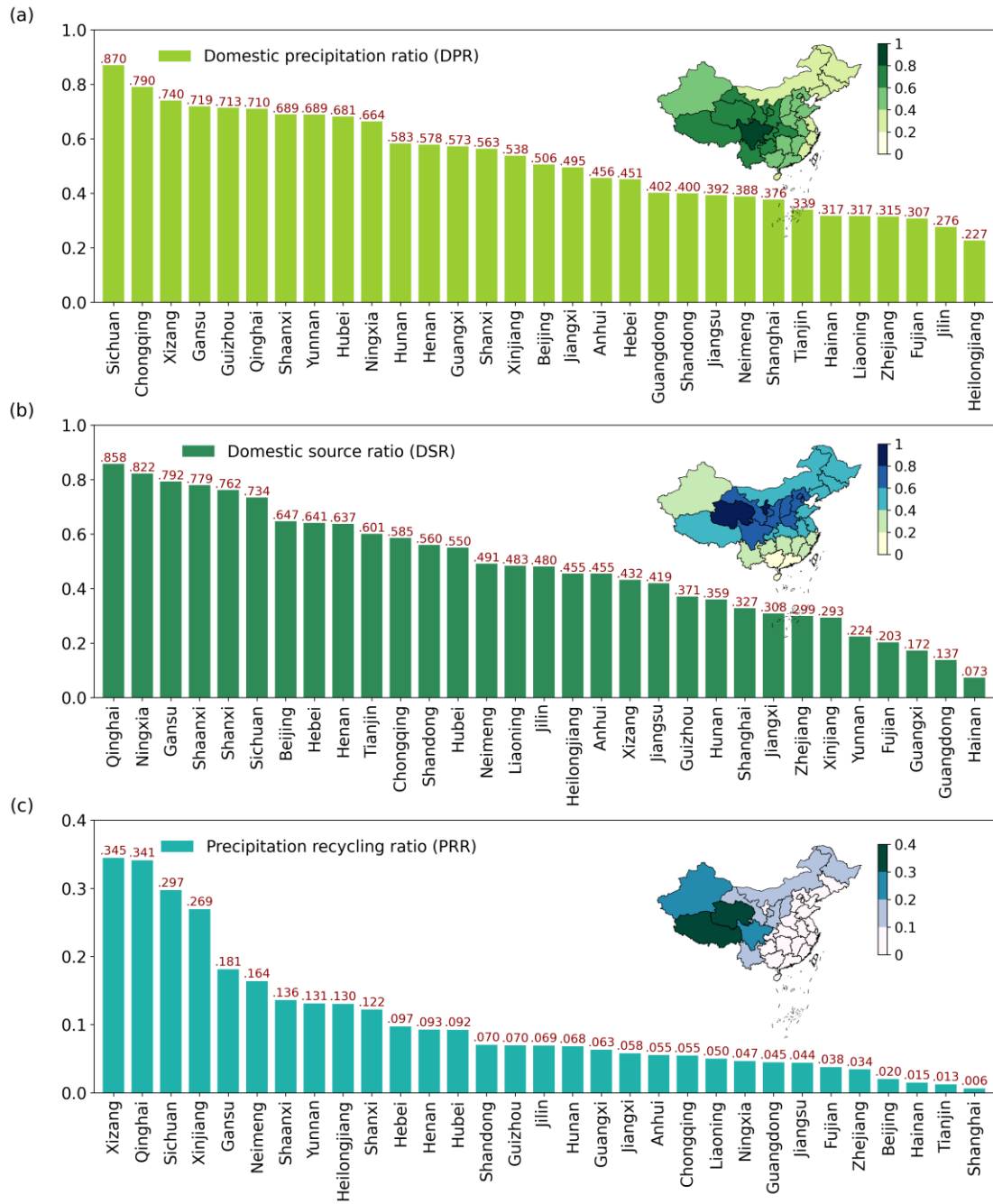
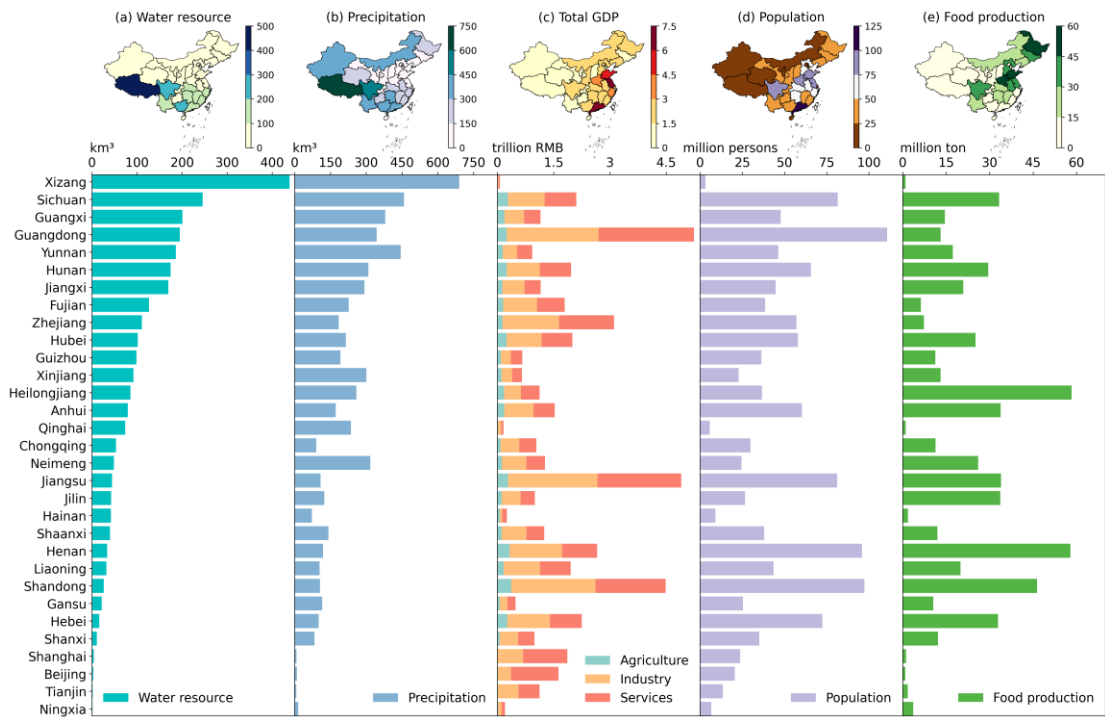


**Figure A2.** (a) Domestic precipitation ratio (DPR), (b) domestic source ratio (DSR) and (c) precipitation recycling ratio (PRR) in each province.

788  
789  
790  
791



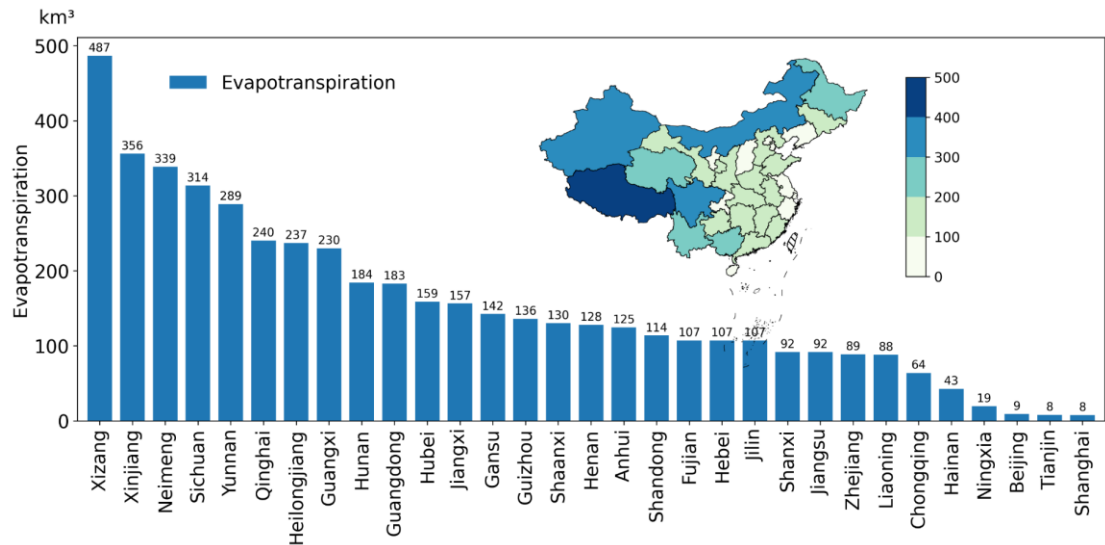
792

793

**Figure A3.** Water resource (a), precipitation (b), GDP (c), population (d) and food production (e) in each province.

794

795

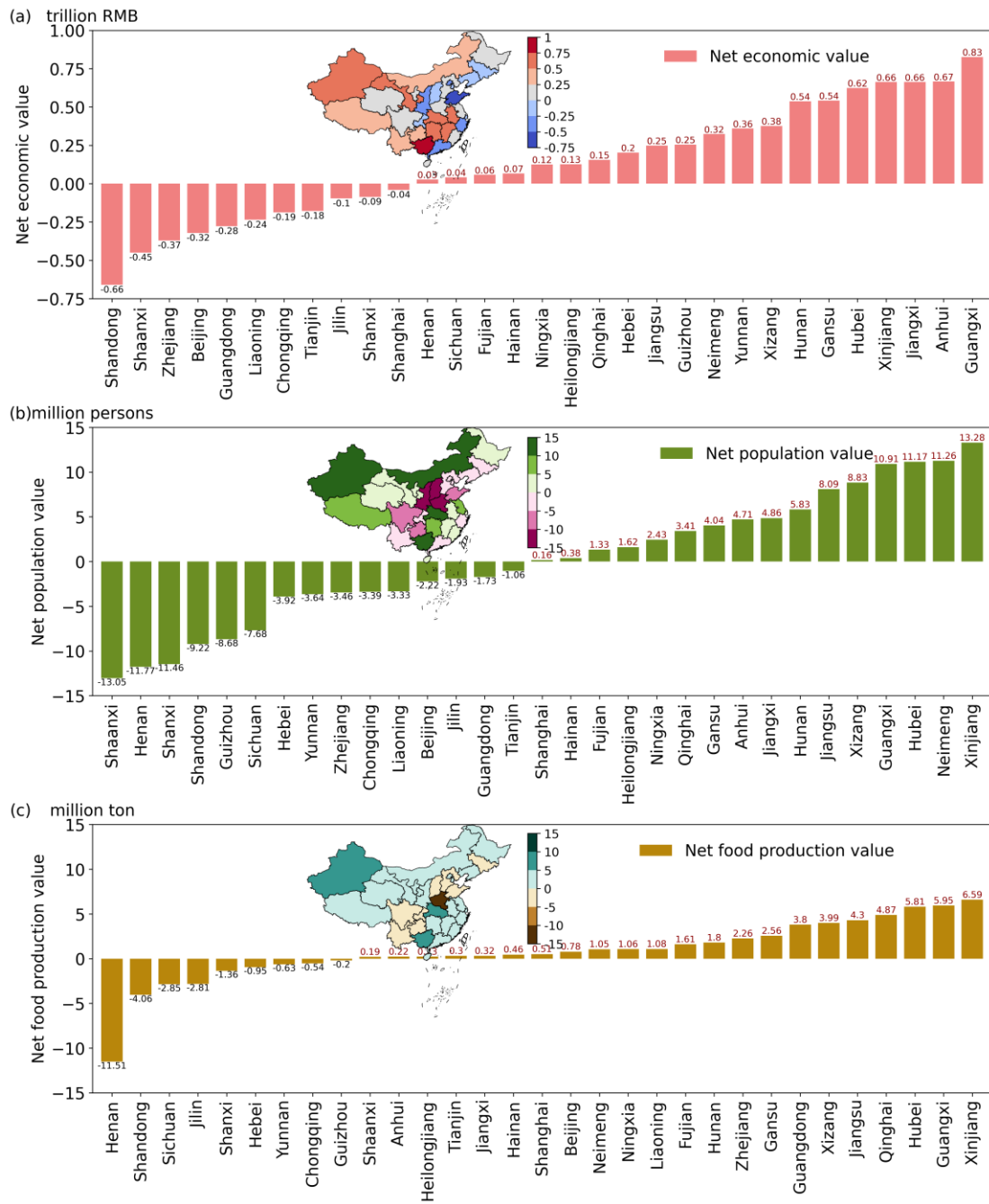


796

797

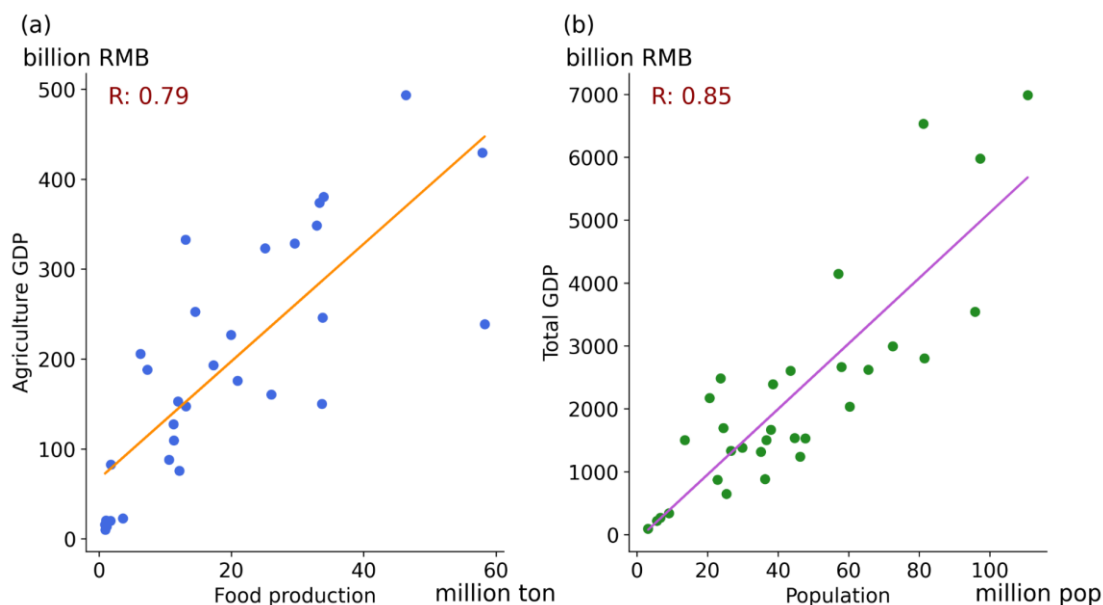
**Figure A4.** Mean evapotranspiration of 2008 to 2017 in each province.

798



799  
800  
801  
802  
803  
804  
805

**Figure A5.** Net GDP (a), population (b), food production (c) value of green water flow in each source province to sink provinces. Positive values represent these socio-economic values of water resource formed by green water increase by flowing from source to sink provinces. Negative values represent these socio-economic values of water resource formed by green water decrease by flowing.



806

807 **Figure A6.** Spatial pearson correlation coefficient between agricultural GDP and food production  
 808 (a), population and total GDP (b) across provinces in China.

809

810 **Table A1.** Precipitation, water resources, and the contribution from green water in provinces of  
 811 China.

Province	Local precipitation (km <sup>3</sup> )	Precipitation formed by green water (km <sup>3</sup> )	Percentage of precipitation contribution to local precipitation (%)	Local water resource (km <sup>3</sup> )	Water resource formed by green water (km <sup>3</sup> )	Percentage of water resource contribution to local water resource (%)
Beijing	9.47	4.53	48	2.82	1.14	40
Tianjin	7.12	2.66	37	1.62	0.70	43
Hebei	100.50	48.35	48	15.98	12.26	77
Shanxi	82.88	51.69	62	10.91	12.38	113
Neimeng	317.11	131.57	41	48.79	31.80	65
Liaoning	104.53	27.80	27	31.92	8.40	26
Jilin	124.15	29.55	24	42.21	8.98	21
Heilongjiang	258.88	53.75	21	85.40	15.44	18
Shanghai	8.02	2.83	35	4.04	1.19	29
Jiangsu	108.09	35.93	33	44.27	13.43	30
Zhejiang	184.72	27.98	15	110.66	13.46	12
Anhui	172.36	56.84	33	79.67	23.19	29
Fujian	226.74	32.96	15	126.39	17.33	14
Jiangxi	292.56	77.52	26	169.44	39.25	23
Shandong	105.99	45.49	43	25.99	13.56	52
Henan	118.83	73.87	62	33.73	24.08	71
Hubei	214.46	108.13	50	101.66	45.27	45

Hunan	308.87	107.25	35	174.33	52.28	30
Guangdong	344.05	73.31	21	194.77	38.54	20
Guangxi	379.82	131.63	35	200.76	66.32	33
Hainan	72.47	13.50	19	41.86	7.13	17
Chongqing	90.61	50.45	56	53.23	21.87	41
Sichuan	458.97	272.93	59	245.86	124.43	51
Guizhou	191.84	97.05	51	98.49	46.54	47
Yunnan	444.68	199.06	45	185.99	96.34	52
Xizang	689.68	360.21	52	438.59	200.33	46
Shaanxi	141.21	89.70	64	39.82	26.14	66
Gansu	115.45	102.36	89	21.60	30.31	140
Qinghai	236.12	170.62	72	73.50	63.57	86
Ningxia	14.95	12.94	87	0.98	3.34	342
Xinjiang	300.10	191.37	64	91.95	64.92	71
Total	6225.19	2683.84	43	2.82	1.14	40

812

813 **Table A2.** The embodied socio-economic values of green water flow from source  
814 provinces for water resources, GDP by industry, population, and food production.

815 Socio-economic indicators are the average value of 2008-2017.

Province	Total GDP (Trillion CNY)	Agriculture GDP (Trillion CNY)	Industry GDP (Trillion CNY)	Service GDP (Trillion CNY)	Population (Million persons)	Food production (Million ton)
Beijing	0.13	0.01	0.05	0.07	2.05	0.97
Tianjin	0.09	0.01	0.04	0.04	1.33	0.61
Hebei	1.27	0.09	0.56	0.62	22	10.82
Shanxi	1.18	0.09	0.54	0.55	22.36	10.35
Neimeng	1.67	0.15	0.77	0.75	30.77	21.78
Liaoning	0.40	0.04	0.19	0.17	7.23	5.92
Jilin	0.27	0.03	0.12	0.11	5.34	6.37
Heilongjiang	0.39	0.05	0.17	0.17	8.04	10.45
Shanghai	0.09	0.01	0.04	0.04	1.41	0.57
Jiangsu	1.06	0.08	0.51	0.47	18.13	8.5
Zhejiang	0.69	0.04	0.32	0.32	11.08	4.11
Anhui	1.37	0.11	0.66	0.59	25.42	11.85
Fujian	0.56	0.04	0.27	0.26	9.46	2.93
Jiangxi	1.33	0.10	0.64	0.59	24.34	9.43
Shandong	1.37	0.11	0.65	0.62	23.85	11.72
Henan	1.75	0.15	0.85	0.75	34.94	16.74
Hubei	1.98	0.18	0.96	0.84	40.57	18.56
Hunan	1.63	0.15	0.78	0.70	33.2	14.13

Guangdong	1.10	0.08	0.52	0.49	20.09	6.38
Guangxi	1.54	0.14	0.73	0.67	33.06	12.7
Hainan	0.18	0.01	0.08	0.08	3.42	1.05
Chongqing	0.66	0.06	0.32	0.28	14.92	6.4
Sichuan	2.31	0.25	1.10	0.96	58.39	24.16
Guizhou	1.08	0.11	0.51	0.46	25.05	10.25
Yunnan	1.48	0.16	0.69	0.63	38.21	14.98
Xizang	0.56	0.07	0.26	0.23	15.32	5.97
Shaanxi	1.48	0.13	0.71	0.64	30.87	14
Gansu	1.05	0.10	0.50	0.46	24.22	10.96
Qinghai	0.72	0.07	0.34	0.31	18.3	7.56
Ningxia	0.18	0.02	0.09	0.08	3.88	1.85
Xinjiang	1.00	0.11	0.46	0.43	22.03	11.6
Total (percentage of total contribution to local socio-economic value)	30.56 (45%)	2.74 (46%)	14.43 (45%)	13.39 (44%)	629.28 (46%)	293.67 (50%)

816